Relationship of Pseudopod Extension to Chemotactic Hormone-Induced Actin Polymerization in Amoeboid Cells

Anne L. Hall, Anthony Schlein, and John Condeelis

Department of Anatomy and Structural Biology, Albert Einstein College of Medicine, Bronx, New York 10461

Aggregation-competent amoeboid cells of *Dictyostelium discoideum* are chemotactic toward cAMP. Video microscopy and scanning electron microscopy were used to quantitate changes in cell morphology and locomotion during uniform upshifts in the concentration of cAMP. These studies demonstrate that morphological and motile responses to cAMP are sufficiently synchronous within a cell population to allow relevant biochemical analyses to be performed on large numbers of cells.

Changes in cell behavior were correlated with F-actin content by using an NBD-phallacidin binding assay. These studies demonstrate that actin polymerization occurs in two stages in response to stimulation of cells with extracellular cAMP and involves the addition of monomers to the cytochalasin D-sensitive (barbed) ends of actin filaments. The second stage of actin assembly, which peaks at 60 sec following an upshift in cAMP concentration, is temporally correlated with the growth of new pseudopods. The F-actin assembled by 60 sec is localized in these new pseudopods.

These results indicate that actin polymerization may constitute one of the driving forces for pseudopod extension in amoeboid cells and that nucleation sites regulating polymerization are under the control of chemotaxis receptors.

Key words: actin, actin-binding proteins, chemotaxis, *Dictyostelium discoideum*

The cellular slime mold *Dictyostelium discoideum* is a popular organism for the study of amoeboid chemotaxis. During vegetative growth single amoeboid cells exist as rapidly-dividing and free-living amoeboid phagocytes which feed on bacteria. These cells are chemotactic to folic acid which is released by bacteria [1]. When the bacterial supply is exhausted the onset of starvation elicits the expression of transmembrane receptors for extracellular cAMP. Subsequent aggregation of cells involves intercellular

signalling and chemotaxis using cAMP that is secreted into the extracellular medium by aggregation-competent cells. The goal of these morphogenetic movements is the formation of a multicellular and species-specific slug which is capable of further differentiation to form the mature, spore-producing fruiting body [2].

Gerisch and his co-workers demonstrated that individual amoeboid cells are capable of chemotaxis toward a localized source of chemoattractant. Using a micropipet to deliver the chemotactic hormone they were able to show that cells respond to chemoattractant initially by extending a pseudopod toward the micropipet [3].

The mechanism by which pseudopod extension occurs in amoeboid cells is unknown. However, in sperm of the sea cucumber *Thyone* [4] and gametes of *Chlamydomonas reinhardii* [5], two simpler eucaryotic cells, the extension of a thin pseudopod (acrosomal process and mating tubule, respectively) is driven in part by actin polymerization from discrete actin nucleation sites that are activated by cell surface signals. In the case of *Chlamydomonas* this is a reversible process which may be relevant to reversible pseudopod extension in amoeboid cells.

The role of actin polymerization in the chemoattractant-stimulated extension of pseudopods in amoeboid cells is unknown. In neutrophils [6,7] and *Dictyostelium* amoebae [8,9] pseudopod extension is correlated with the appearance of dense microfilament networks at sites of pseudopod growth.

In neutrophils increases in F-actin content have been correlated with changes in right-angle light scattering and cell shape that occur in response to chemotactic stimulation [10,11]. Since chemotactic stimulation also elicits pseudopod extension in neutrophils [12], it is possible that actin polymerization is driving pseudopod growth. However, the relationship between actin polymerization and pseudopod extension in neutrophils remains obscure due to an incomplete understanding of the relative kinetics of these two processes.

In *D. discoideum* the amount of actin in Triton X-100-resistant cytoskeletons prepared from amoebae increases if cells are first stimulated with chemoattractants [13]. However, it is not clear whether such increases are due to polymerization of actin or filament cross-linking and whether these increases occur prior to or during cell lysis [14]. Furthermore, the kinetics of pseudopod extension during stimulation of amoeboid cells with chemoattractant has not been well established [15,16,20].

In this study we have investigated the kinetics of pseudopod extension, changes in F-actin content, and the location of F-actin in whole cells during stimulation of aggregation-competent amoebae of *D. discoideum* with cAMP.

MATERIALS AND METHODS

Materials

Culture media included Bacto-peptone, Bacto-agar, Bacto-peptamin, Proteose Peptone (Difco), and yeast extract (BBL Microbiology Systems); CAMP was purchased from Sigma or Boehringer Mannheim and stored in solution as a 10^{-4} M stock with 10 mM PIPES, pH 6.7, at $-20°C$. OsO_4 and EM grade glutaraldehyde were purchased from Polysciences. A concentrated 18.2 μM stock of NBD-phallacidin (Molecular Probes, Inc.) was prepared by drying under prepurified N_2. Heat-inactivated fetal calf serum (FCS) (Gibco) and Pentex bovine albumin fraction V (BSA) (Miles Scientific) were used during actin localization. The specificity of the antiactin antibody that was used in these studies has been described elsewhere [17,18]. Rhodamine-labelled sheep antirabbit

IgG (Gibco) was prepared by preabsorption against whole *Dictyostelium* lysate. Other chemicals used included N-propyl gallate (Kodak), 37% formaldehyde solution (Fisher), absolute methanol (MeOH) (Baker), and cytochalasin D (Sigma). A 20 mM cytochalasin stock was prepared in DMSO and stored at $-20°C$. A caffeine stock (100 mM in deionized H_2O) was prepared fresh for each experiment. Deionized H_2O was obtained after processing by a Barnstead 120V Nanopure-A System and passage through a 0.2-μm filter.

Cells

Strain NC4 was grown in association with *Klebsiella aerogenes* on SM/5 or SM agar (SM agar 1% α-D:(+)glucose, 1% Bacto-peptone, 4 mM $MgSO_4$, 20 mM KPO_4, 0.1% yeast extract, 1.5% Bacto-agar, pH 6.4). Strain AX3 was grown in HL5 medium (1% α-D(+)-glucose, 0.5% yeast extract, 0.5% Proteose Peptone, 0.5% Bacto-pep-tamin, 2.5 mM Na_2HPO_4, 2.6 mM KH_2PO_4, 35 μM dihydrostreptomycin sulfate, pH 6.4) in Ehrlenmeyer flasks on a rotary platform shaker at 175 rpm (culture volumes were approximately 1/5 the capacity of the flask). Cells were harvested at late log phase. NC4 cells were rinsed off of growth plates with sterile salt solution (10 mM NaCl, 10 mM KCl, 2.7 mM $CaCl_2$, pH 6.4). AX3 cultures were simply poured into centrifuge tubes. All cells were washed twice by centrifugation (4 min, 150g each) and suspended in buffer to initiate development. The buffer used for video microscopy and scanning electron microscopy preparations was HPDF (10 mM KCl, 20 mM $NaPO_4$, 0.35 mM $CaCl_2$, 1 mM $MgSO_4$, 34 μM dihydrostreptomycin sulfate, pH 6.4). MES/Na buffer (20 mM MES, 0.2 mM $CaCl_2$, NaOH to pH 6.4) was used for actin localization and the NBD-phallacidin binding assay. The temperature was maintained at 21°C during culture growth and all procedures.

Video Microscopy and Analysis

NC4 cells were placed in a Sykes-Moore chamber at 6 hr of development and perfused with buffer at 4 ml/min to prevent cAMP-dependent signal relay between cells. At 0 sec a square-wave pulse of 10^{-6} M cAMP was injected in the chamber for 1 min at the same flow rate. Amoeboid movement was recorded in real time with a video system and a Zeiss Universal microscope with phase optics. Videotapes were analyzed manually for velocity of locomotion and graphed as microns/sec. The asymmetry index (AI) was calculated by measuring the perimeter of each cell with a touch pad planimeter, calculating the corresponding area, and dividing this area by the area of the same cell if it were circular. The AI equals 1.0 for a round cell and increases in value as the cell becomes more asymmetric.

Scanning Electron Microscopy

NC4 cells were prepared for scanning electron microscopy as described in Condeelis et al. [19] except that cells were exposed to 10^{-6} M cAMP or buffer for various times before replacement of the covering solution by 1% OsO_4 in buffer (processing of pre-stimulation samples did not incude this additional step).

Quantitation of these cell populations was done by scoring cells as amoeboid or rounded at a magnification of 260×. The results were confirmed in a double-blind test.

NBD-Phallacidin Binding Assay

The change in F-actin content following cAMP stimulation was quantitated with an NBD-phallacidin binding assay modified from that of Howard and Oresajo [10]. AX3 cells at 10^7/ml were monitored for changes in light scattering starting at 3.5 hr of development. Cells were pumped through a flow cell at 7 ml/min from a beaker on an orbital shaker (110 rpm) and the transmittance at 470 nm was monitored by a Gilford spectrophotometer (model 250). At 4 hr of development cells were stimulated once by adding 0.01 volume of 10^{-4} M cAMP stock (10^{-6} M cAMP final). Seven minutes later caffeine was added to final 3 mM from 100 mM stock. Commencing 30 min after addition of caffeine, samples were fixed before and after stimulation with 10^{-6} M cAMP or 10 mm PIPES pH 6.7 by withdrawing aliquots of 2.5 × 10^6 cells and adding them to 1.5-ml Eppendorf tubes containing 0.1 ml 37% formaldehyde solution, 0.75 ml 2 × fix buffer (0.2% Triton X-100 in 2 × general buffer (GB) (GB: 20 mM KPO_4, 10 mM PIPES, 5 mM EGTA, 2 mM $MgSO_4$, pH 6.8) and deionized H_2O so that the final fixation volume was 1.5 ml. Samples were fixed for 15 min on a rotator and centrifuged for 1 min at 12,000g, and the supernates were discarded. The pellets were resuspended by vortexing in saponin buffer (0.1% saponin, 20 mM KPO_4, 10 mM PIPES, 5 mM EGTA, 2 mM $MgSO_4$, pH 6.8) and stained 1 hr with 0.3 μM NBD-phallacidin on a rotator. Samples were centrifuged as above and washed once with saponin buffer. NBD-phallacidin was extracted from the cell pellets in 0.5 ml MeOH for 30 min on the rotator. Samples were centrifuged 1 min at 12,000g; the destained cell pellet was discarded; and the emitted fluorescence of the supernates was read in a 1.0-ml capacity, 10-mm-pathlength cuvette by a Perkin-Elmer MPF-3L fluorometer at 465-nm excitation, 535-nm emission. Relative F-actin content is the ratio of the percent emission of a cAMP-stimulated sample divided by the percent emission of a buffer-stimulated sample.

The total actin content of cells was calculated from the densitometry data of Eckert et al. [27]. The percent of F-actin was calculated from the NBD-phallacidin binding assay by using a K_d of 2 × 10^{-8} M for the binding of NBD-phallacidin to F-actin [44]. Under our conditions, greater than 94% of the NBD-phallacidin binding sites associated with F-actin in cells were occupied by NBD-phallacidin during the assay.

Cytochalasin D Treatment

AX3 cells at 10^7/ml were treated with cytochalasin D for 15 min prior to stimulation and fixation for the NBD-phallacidin binding assay. Cytochalasin D was added to the Eppendorf tubes before addition of cells when necessary so that its final concentration was equivalent in all tubes during fixation.

Actin Localization

The subcellular distribution of actin was determined by using indirect immunofluorescence with antiactin and NBD-phallacidin staining of intact cells. NC4 cells were prepared as for scanning electron microscopy with the addition of 3 mM caffeine for 0.5 hr prior to sample preparation. At the point at which OsO_4 was used for SEM preparations, 1% glutaraldehyde and 0.1% Triton X-100 were substituted and the cells were fixed for 5 min, followed by three washes of 7 min each with 1 mg/ml $NaBH_4$ in GB (buffer was added to solid $NaBH_4$ less than 30 sec before use in a wash). This procedure yields the best preservation of cell appearance, as judged by phase microscopy, with no remaining artifactual fluorescence induced by glutaraldehyde, as judged by

inspection at 450–490 nm (rhodamine filter) and 510–560 nm (fluorescein filter) using a Zeiss Universal Microscope equipped with Epi-fluorescence condensor III RS. Non-specific staining was blocked by treatment with 1% (FCS) in staining solution (1% BSA in TBS (0.9% NaCl, 20 mM Tris-Hcl, 0.02% NaN_3, pH 7.8)) for 15 min. Staining with 5 µg/ml affinity-purified antiactin polyclonal antibody or 0.3 µM NBD-phallacidin in staining solution lasted 45 min and was followed by three rinses, 5 min each, in 0.1% BSA and 0.02% saponin in TBS. Samples treated with antibody were further stained for 45 min with rhodamine-labelled sheep antirabbit IgG diluted 1:1,000 in the staining solution and then rinsed as above in 0.1% BSA and 0.02% saponin in TBS. All coverslips were mounted with 0.1 M N-propyl gallate in 50% glycerol-PBS (PBS: 4.5% NaCl, 20 mM $NaPO_4$, 0.02% NaN_3, pH 7.0). Cells were examined as above with phase inter-ference and epifluorescence optics. Samples prepared without primary and/or without secondary antibody were not fluorescent.

RESULTS

To investigate the relationship between pseudopod extension and actin polymeri-zation during chemotactic stimulation it was first necessary to determine the kinetics of pseudopod extension in response to chemoattractant and then to determine whether the responses of cells to chemotactic stimulation are synchronous enough to permit correlation of cell morphology with biochemical analysis of F-actin content.

Analysis of the Morphological Response

Futrelle and co-workers [20] have demonstrated that a pulse of cAMP will cause aggregation-competent cells to "cringe" (round up) within 30 sec followed by a return to normal locomotion. In order to define the kinetics of this response with more precision, to determine if additional morphological changes occur, and to investigate the synchrony
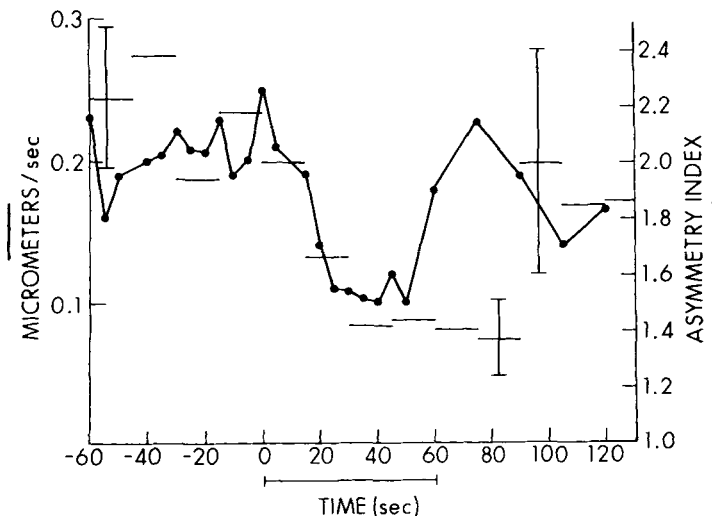

Fig. 1. Response of cells to a 1-min pulse of cAMP (|——|). Horizontal lines indicate the average velocity of cells over each 15-sec time interval indicated; ●——● is the asymmetry index. N = 91. Error bars indicate the standard deviation for velocity of locomotion.

of these responses, cells were stimulated with square-wave pulses of cAMP of known duration. Videotape analysis of cells stimulated in a Sykes-Moore chamber (Fig. 1) demonstrates that cells respond to an upshift in cAMP by decreasing their rate of locomotion and rounding (cringing), which involves pseudopod withdrawal. Both responses peak within 25 sec of the beginning of the cAMP pulse. These results confirm the analysis of Futrelle et al. [20] and Klein et al. [40].

However, an additional morphological change was observed. After cringing the cells undergo a dramatic increase in asymmetry, beginning between 50 and 60 sec, that is shown by scanning electron microscopy to involve extension of pseudopods (ruffles, filopods, lobopods) from the entire cell surface (Fig. 2). Therefore, pseudopod extension is responsible for the increase in asymmetry described by us (Fig. 1) and possibly the increase in cell area reported by others [16] using phase microscopy.

The cells do not increase their rate of locomotion during this phase of the response to cAMP, but by 120 sec they have returned to the prestimulus morphology and rate of locomotion (Fig. 1). The cells appear to be responding to the initial upshift in cAMP concentration since similar results were obtained regardless of the duration of the pulse of cAMP.

The synchrony of morphological change of the cell population during the cAMP pulse was determined by quantitative morphometry (Fig. 3). Preparations such as those shown in Fig. 2 were used to count the number of cells that were amoeboid (i.e., with pseudopods of various types) or round (cringed) at each time point. Control preparations
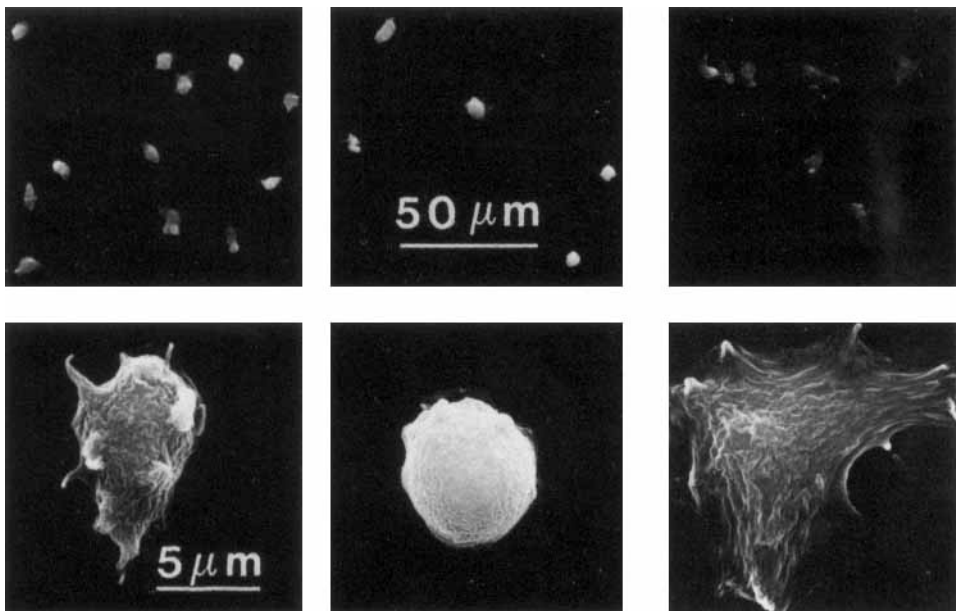

Fig. 2. Scanning electron microscopy of a cell preparation that was identical to those analyzed in Fig. 1. The cells were rapidly fixed in 1.0% OsO_4 at the times indicated following a uniform upshift in cAMP concentration from zero to 10^{-6} M. **Left:** cells fixed 30 sec before stimulation with cAMP; **middle and right:** 25 sec and 60 sec after addition of 10^{-6} M cAMP. The top row shows fields of cells ($\times 260$), while each photo on the bottom shows a representative cell of each population at higher magnification ($\times 5,400$). Photos in each row are at identical magnifications as indicated.
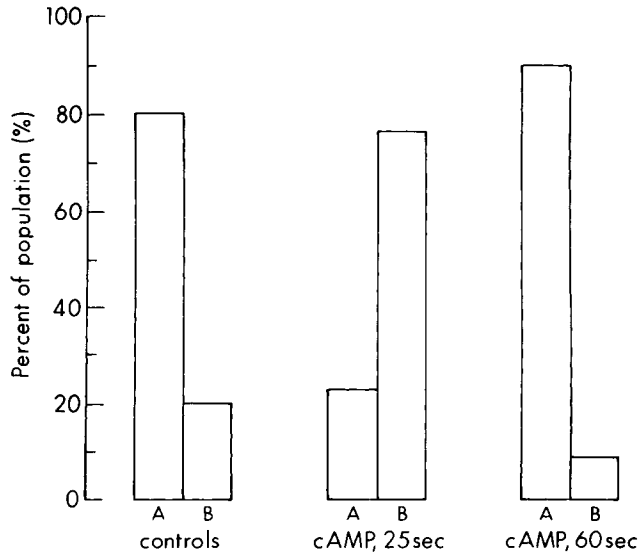
Fig. 3. Quantitation of cell morphology after fixation at the times indicated following stimulation with cAMP as described for Fig. 2. **A:** Cells with projections. **B:** Rounded cells. Populations of cells from the three types of control preparations listed in the text were indistinguishable from one another and the data were pooled in the "control" category. Controls, $N = 2,481$ cells; 25 sec after cAMP, $N = 503$; 60 sec after cAMP, $N = 706$.

were pulsed with buffer in the absence of cAMP or fixed at 60 sec or 30 sec before the cAMP pulse without any buffer pulse.

In all control samples 80% of the cells are amoeboid while only 20% are rounded. However, in samples fixed 25 sec after the beginning of the cAMP pulse only 20% of the cells are amoeboid while about 80% are rounded. By 60 sec following the cAMP upshift over 90% of the cells have extended pseudopods while very few remain rounded.

These results demonstrate that cAMP induces a phase of synchronous pseudopod extension which begins, as detected by phase microscopy, between 50 and 60 sec following the upshift in cAMP concentration.

Measurements of Actin Polymerization

In order to determine if actin polymerization is correlated with any of the morphological changes that are stimulated by cAMP, the F-actin content of cells was measured by using an NBD-phallacidin binding assay.

Figure 4 demonstrates that cAMP induces rapid and substantial increases in F-actin content. Within 10 sec after beginning the cAMP upshift there is a sharp increase in F-actin content. This increase just precedes the cringe response in Figure 1. F-actin then drops back almost to its original level by 20 sec during the "cringe" response. This is followed by a large increase in the cell content of F-actin, beginning at about 30 sec and peaking at 60 sec, which corresponds to the time during which cells extend pseudopods. The cellular content of F-actin then slowly falls back to prestimulation levels by 7 min.

These values for the relative F-actin content correspond to 35–40% F-actin in cells before stimulation and 55–65% F-actin in cells following stimulation with cAMP. It
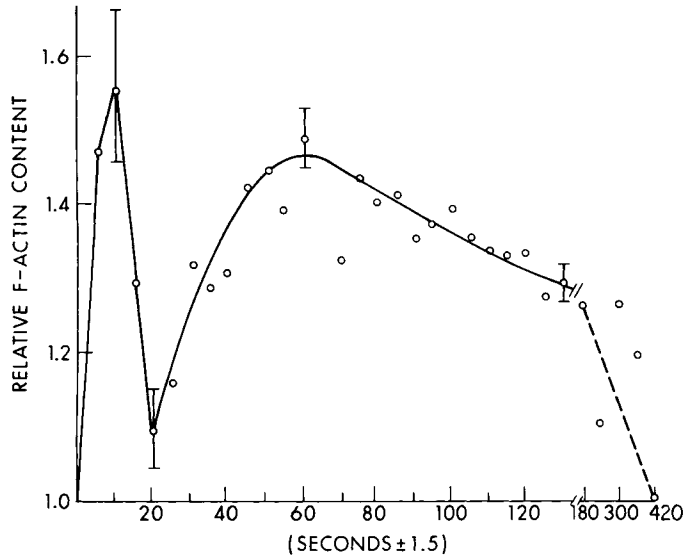
Fig. 4. The content of F-actin in cells was measured by using the NBD-phallacidin binding assay described in Materials and Methods. At 0 sec a rapid upshift from 0 to 10^{-6} M cAMP was begun. Each point represents the average of four to six experiments. Error bars shown at inflection points are standard deviations.

should be noted that these values were calculated for cells that had been treated with caffeine before the start of the experiment to inhibit adenylate cyclase and prevent spontaneous cAMP release and signalling [45]. Such treatment reduces the percent F-actin in unstimulated cells by as much as 50% (Hall and Condeelis, unpublished observations).

Dose-dependent response curves of cAMP-stimulated increases in F-actin content are shown in Figure 5. The first peak of F-actin, which occurs between 5 and 10 sec following the cAMP upshift, appears to peak at a slightly higher concentration of cAMP than does the 60-sec peak. However, the standard deviations suggest that these two dose-response curves may not be significantly different.

Cytochalasin D Sensitivity

To determine if increases in F-actin content were due to polymerization of actin filaments by addition of monomers to the barbed ends of filaments, cells were treated with cytochalasin D. As shown in Figure 6, cytochalasin D inhibits cAMP-stimulated increases in F-actin content at all time points measured. The cytochalasin D concentration required for half-maximal inhibition was calculated to be 5 μM at 5–10 sec, 2.5 μM at 50–60 sec, and 4 μM at 80–90 sec followiong the cAMP upshift. Concentrations of cytochalasin D above 10 μM actually increased the F-actin content of both control and cAMP-stimulated cells so that concentrations higher than 5 μM were not used in experiments designed to measure inhibition of actin polymerization. This latter effect possibly results from the cytochalasin-induced nucleation of actin assembly which occurs at higher concentrations of cytochalasin [41].
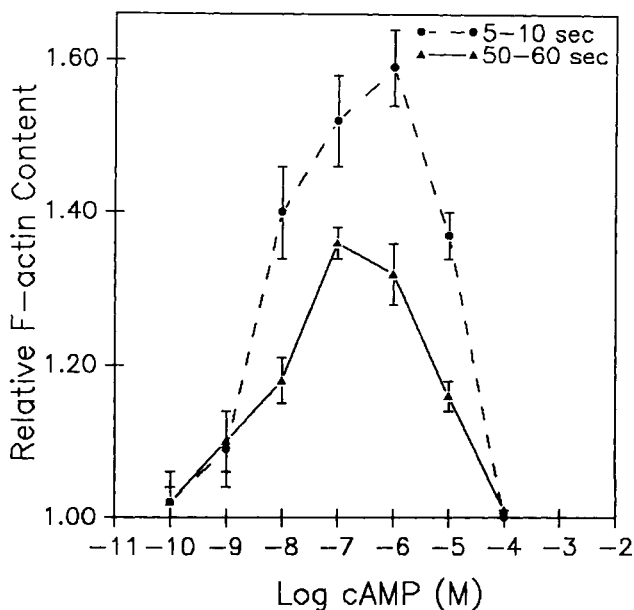
Fig. 5. Cyclic AMP dose-response curves of F-actin content for time points between 5 and 10 sec and 50 and 60 sec. Each point represents the average of three experiments. Error bars indicate standard deviations.
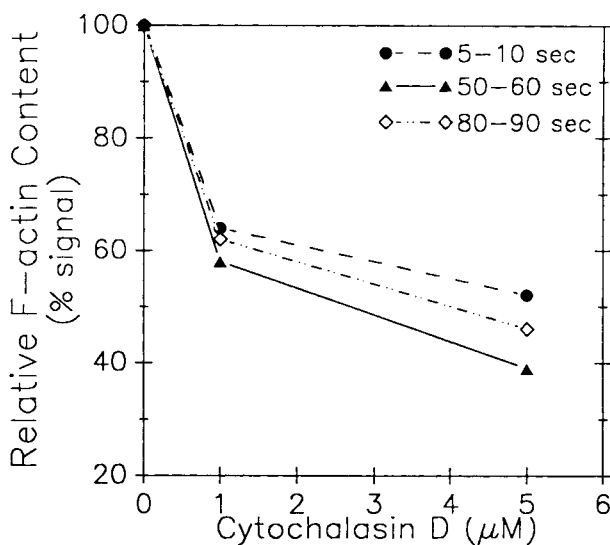

Fig. 6. Cytochalasin D inhibits cAMP-stimulated increases in F-actin content. F-actin content was measured with the NBD-phallacidin binding assay in cytochalasin D-treated and -untreated cells. Both treated and untreated cells were in the presence of 1% DMSO for the time of treatment and the final concentration of cytochalasin D during fixation was the same in all samples. Measurements were made at time points between 5 and 10 sec, 50 and 60 sec, and 80 and 90 sec following an upshift in cAMP concentration from 0 to 10^{-6} M.

Location of F-Actin Which Is Assembled in Response to Chemotactic Stimulation

The above results demonstrate that the accumulation of F-actin which peaks at 60 sec following cAMP stimulation is temporally correlated with the extension of new pseudopods. To investigate the location of F-actin relative to that of total actin (filamentous and nonfilamentous) in cells during stimulation with cAMP, cells were fixed 30 sec before (-30 sec) and 25 and 60 sec following an upshift in cAMP concentration from zero to 10^{-6} M. Cells were then stained with a polyclonal antiactin antibody that recognizes both G- and F-actin [17,18] and a rhodamine-labelled secondary antibody, or with NBD-phallacidin, which binds only to F-actin. Figures 7 and 8 show that total actin is present in the cell center as well as being concentrated in pseudopods while F-actin is concentrated in pseudopods at -30 sec. These results are consistent with studies
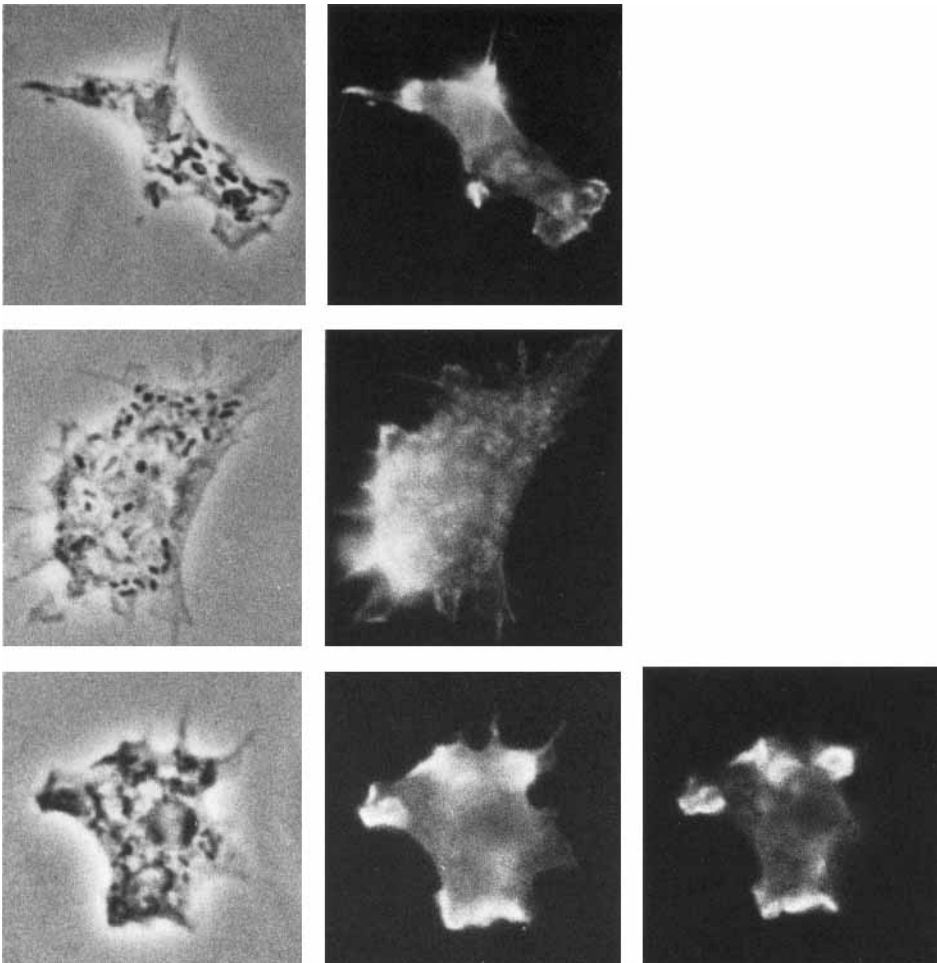

Fig. 7. *Immunofluorescence with an antiactin antibody which recognizes both G- and F-actin demonstrates that total actin is present in cell body, cortex, and pseudopods both before and after stimulation with cAMP.* **Top:** unstimulated amoeboid cell; **middle:** 60 sec after stimulation; **bottom:** 60 sec after stimulation but showing two planes of focus. ×2,100.
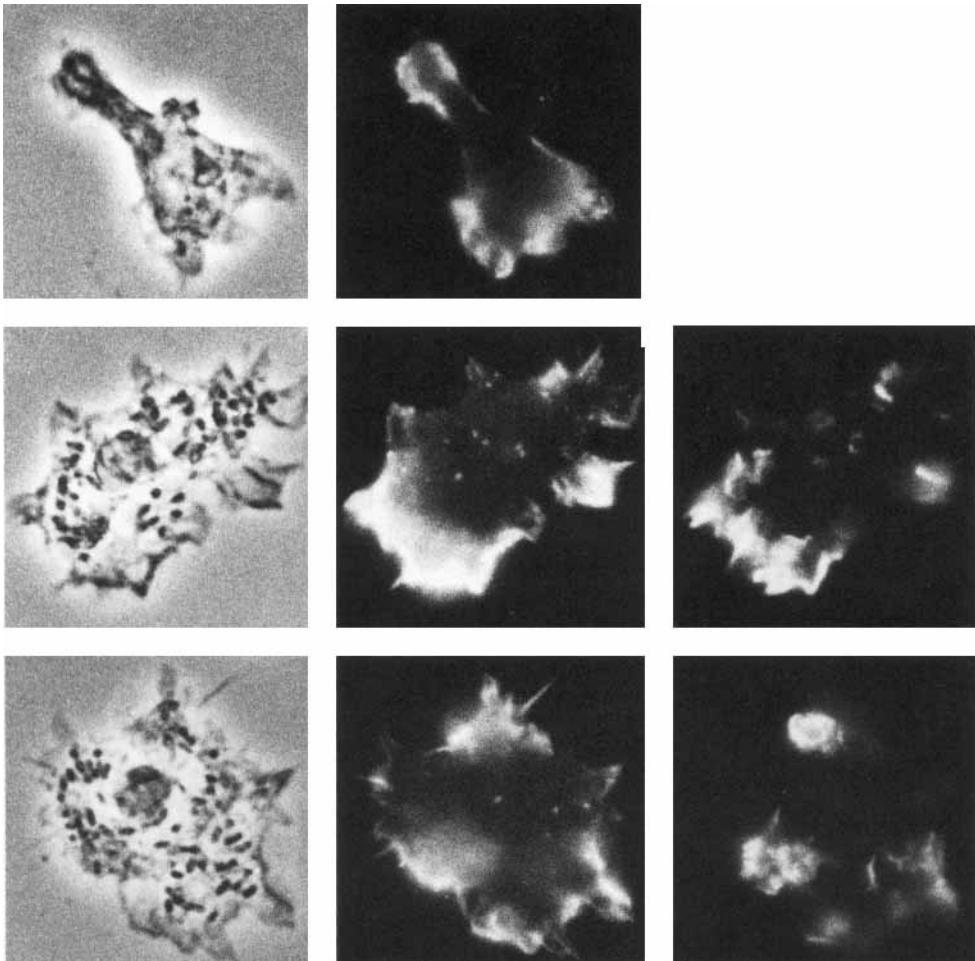
Fig. 8.   Fluorescence light microscopy with NBD-phallacidin detects F-actin predominantly in pseudo-pods indicating that the F-actin which is assembled by 60 sec following cAMP stimulation is in the new pseudopods. **Top:** unstimulated amoeboid cell; **middle, bottom:** 60 sec after stimulation showing two planes of focus. ×2,100.

demonstrating the presence of actin [18,42] and F-actin [28] in pseudopods during unstimulated random amoeboid locomotion. Twenty-five seconds following cAMP stim-ulation cells are spherical and exhibit uniform fluorescence when stained for either total actin or F-actin (not shown). The intensity of NBD-phallacidin staining for F-actin in cells at 25 sec is approximately equal to that in cells which have not been stimulated (Fig. 4).

Cells fixed 60 sec following the cAMP upshift exhibit similar differences in the locations of total actin and F-actin. While total actin is found in the cell center as well as in pseudopods (as in unstimulated samples), F-actin is concentrated predominantly in the numerous new pseudopods that have been extended by 60 sec. Furthermore, the intensity of staining with NBD-phallacidin is approximately 1.5 times greater in cells at 60 sec than that in unstimulated cells (Fig. 4). This is the first time that the distribution

of actin and F-actin has been demonstrated during the stimulation of pseudopod extension by chemoattractants.

DISCUSSION

The studies reported in this paper demonstrate that morphological and motile responses to a uniform upshift in the concentration of the chemotactic hormone cAMP are sufficiently synchronous within a cell population to allow relevant biochemical analyses to be performed on large numbers of cells.

Measurements of the F-actin content of cells using the NBD-phallacidin binding assay demonstrate that increases in F-actin occur in two stages following stimulation of cells with cAMP. Both increases in F-actin content are inhibited by cytochalasin D, indicating that each involves actin polymerization by the addition of monomers to barbed ends of filaments.

These two stages can be distinguished in several ways, however, and are correlated with different physiological events that occur following stimulation with cAMP. The peak of F-actin content at 10 sec occurs and then decays while cells are beginning to withdraw pseudopods, leading to the so-called "cringe" morphology. The second peak of F-actin, at 60 sec, is correlated with the growth of new pseudopods, leading to amoeboid morphology.

Peaks in F-actin content at 10 and 60 sec exhibit slightly different sensitivities to cAMP and cytochalasin D. At 10 sec the optimum increase in F-actin content occurs at 1×10^{-6} M cAMP while the 60-sec peak is optimum at 1×10^{-7} M cAMP. The cytochalasin concentration required for half-maximal inhibition of the actin response is 2.5 μM at 50–60 sec and 5 μM at 5–10 sec after cAMP stimulation.

Furthermore, dephosphorylation of the myosin II heavy chain occurs until 30 sec following cAMP stimulation and is followed by phosphorylation of the heavy chain which peaks at 60 sec [23]. In vitro studies have shown that dephosphorylation potentiates the polymerization of myosin thick filaments while phosphorylation favors depolymerization [24,25]. Thick filament formation is correlated with contractility [26] which may stimulate the polymerization of actin [27]. These results suggest that at least a fraction of the peak of actin assembly occurring at 10 sec may result from a contraction, mediated by myosin thick filaments, that eventually leads to cell rounding at 20 sec. On the other hand the 60-sec peak of actin assembly is cotemporal with myosin heavy chain phosphorylation, which suggests that this peak of actin assembly is not the result of myosin-mediated contraction but may result from a separate signalling pathway.

However, preliminary evidence indicates that neither peak of F-actin assembly is inhibited by pretreatment of cells with pertussis toxin in the range of concentrations that inhibit chemotaxis in neutrophils [21,22].

Together these observations suggest that the peak of actin assembly at 60 sec following stimulation with cAMP is specifically related to the reorganization of the actin cytoskeleton that results in pseudopod extension at this time.

Does Actin Polymerization Drive Pseudopod Extension?

Comparison of the fluorescence patterns obtained when cells are stained for total actin with those of cells that are stained for F-actin demonstrates that F-actin, which is assembled by 60 sec following stimulation with cAMP, is concentrated within new pseudopods while total actin (G + F), in addition to being concentrated in pseudopods,

is also present in the cell center at this time. This suggests that F-actin assembly is occurring primarily at the sites of pseudopod extension and not throughout the cell center. This raises the possibility that pseudopod extension is driven, independent of the action of myosin, by the polymerization of actin at the site of pseudopod extension as occurs in several simpler eukaryotic cells [4,5].

Several laboratories have shown by immunofluorescence [26,28] that pseudopods of *Dictyostelium* amoebae do not contain myosin. We have demonstrated that pseudopod extension does not require the presence of myosin at the site of initial pseudopod growth [18].[1]

The formation of a new pseudopod appears to require cross-linking of actin filaments. Chemotactic stimulation of *Dictyostelium* amoebae results in an increase in the amount of actin associated with Triton X-100 cytoskeletons isolated by centrifugation at low g-forces [13]. These are conditions under which F-actin alone will not sediment, thus suggesting that increases in cross-linking of actin filaments to form large aggregates has occurred in response to chemotactic stimulation.

Furthermore, ABP-120, an actin-binding protein from *D. discoideum* that cross-links actin filaments to form orthogonal networks in vitro [9,29,30] is concentrated in pseudopods of both unstimulated [31] and stimulated cells [32]. Electron microscopy demonstrates that microfilaments present in pseudopods of *Dictyostelium* amoebae are organized primarily in an orthogonal network similar in appearance to networks assembled in vitro with purified ABP-120 and actin [9].

Based on these considerations we propose that pseudopod extension during chemotactic stimulation results from site-specific polymerization of actin filaments and their accumulation (by 60 sec in these experiments) in the cell cortex. Cross-linking by cortical actin-binding proteins such as ABP-120 would result in assembly of a viscoelastic gel that could increase in volume due to hydration and further polymerization. The resulting expansion of the cell cortex would lead to the formation of a pseudopod. In this model local actin polymerization would be regulated by the chemotaxis receptor in response to cAMP binding. Receptor regulation is supported by the cAMP dose-response curves for actin assembly in vivo (Fig. 5) which are similar to the dose-response curves measured for chemotaxis [33].

Actin polymerization that is stimulated by occupied chemotaxis receptors might be mediated by nucleation sites analogous to those observed in *Thyone* sperm [4] or *Chlamydomonas* [5] which regulate site-specific actin polymerization in response to cell surface signals. In amoeboid cells, however, such nucleation sites will of necessity be globally distributed to support multidirectional extension of pseudopods that occurs in uniform upshifts of chemoattractant (Fig. 2) or during sequential stimulation of different regions of the cell surface [34].

The identity of the nucleation sites in amoeboid cells remains a mystery. Our finding that the 5–10-sec peak of actin assembly has lower sensitivity to cytochalasin D than the 50–60-sec peak is consistent with the insensitivity to cytochalasin B of the first peak of accumulation of actin in triton cytoskeletons following chemotactic stimulation [14]. These results suggest that the initial polymerization of actin following hormone stimulation may involve a step at which the barbed ends of actin filaments are blocked to either actin monomer or cytochalasin addition. The involvement of calcium-regulated capping proteins like gelsolin [35,36] or severin [37] at this step might be

[1]Ogihara et al., manuscript submitted.

crucial in nucleating the growth of filaments that are blocked at the barbed end [43]. However, any model for nucleation of filament assembly involving these proteins must account for the observation that calcium, which is required for the severing and nucleation activity of gelsolin and severin, does not appear to be sufficient to stimulate actin polymerization in either neutrophils [11,38] or saponin-permeabilized *Dictyostelium* amoebae [39] at physiological concentrations.

Further study of the regulation and composition of the actin nucleation activities involved in amoeboid chemotaxis will require the exploitation of in vitro models that exhibit physiological responsiveness to chemotactic hormones. Such models are currently under development in our laboratory.

ACKNOWLEDGMENTS

REFERENCES

1. Pan P, Hall E, Bonner JT: Nature New Biol 237:181, 1972.
2. Loomis WF: "The Development of *Dictyostelium discoideum*." New York: Academic Press, 1982.
3. Gerisch G, Malchow D, Huesgen A, Nanjundiah V, Roos W, Wick U: In McMahon D, Fox CF (eds): ICN-UCLA Symposium on Developmental Biology 2:76, 1975.
4. Tilney L: J Cell Biol 77:551, 1978.
5. Detmers P, Goodenough U, Condeelis J: J Cell Biol 97:522, 1983.
6. Malech HL, Root RK, Gallin JI: J Cell Biol 75:666, 1977.
7. Ryder KI, Weinreb RN, Niederman R: Anat Rec 209:7, 1984.
8. Condeelis J: In Schweiger H (ed): "International Cell Biology." Berlin: Springer-Verlag, 1981 p 306.
9. Wolosewick JJ, Condeelis J: J Cell Biochem 30:227, 1986.
10. Howard T, Oresajo C: J Cell Biol 101:1078, 1985.
11. Sklar L, Omann G, Painter R: J Cell Biol 101:1161, 1985.
12. Zigmond S, Sullivan S: J Cell Biol 82:517, 1979.
13. McRobbie SJ, Newell PC: Biochem Biophys Res Commun 115:351, 1983.
14. McRobbie SJ, Newell PC: Exp Cell Res 160:275, 1985.
15. Chisholm RL, Fontana D, Theibert A, Lodish HF, Devreotes P: In Losick R, Shapiro L (eds): "Microbial Development." Cold Spring Harbor: Cold Spring Harbor Laboratories, 1985, p 219.
16. Fontana D, Wong T-Y, Theibert A, Devreotes P: In Steinberg M (ed): "The Cell Surface in Cancer and Development." New York: Plenum Publishing, 1985, p 261.
17. Carboni JM: "The Cell Cortex of *Dictyostelium Discoideum*: A Dynamic Actin-Containing Compartment." Ph.D. Thesis. New York: Albert Einstein College of Medicine, 1984.
18. Carboni JM, Condeelis JS: J Cell Biol 100:1884, 1985.
19. Condeelis J, Ogihara S, Bennett H, Carboni J, Hall A: Methods Cell Biol 28:191, 1987.
20. Futrelle RP, Traut J, McKee WG: J Cell Biol 92:807, 1982.
21. Becker EL, Kermode JC, Naccache PH, Yassin R, Marsh ML, Munoz JJ, Sha'afi RI: J Cell Biol 100:1641, 1985.
22. Spangrude GJ, Sacchi F, Hill HR, Van Epps DE, Daynes RA: J Immunol 135:4135, 1985.
23. Berlot CH, Spudich JA, Devreotes PN: Cell 43:307, 1985.
24. Berlot CH, Devreotes PN, Spudich JA: J Biol Chem 262:3918, 1987.
25. Kuczmarski ER, Spudich JA: Proc Natl Acad Sci USA 77:7292, 1980.
26. Yumura S, Fukui Y: Nature (Lond) 314:194, 1985.
27. Eckert BS, Warren RH, Rubin RW: J Cell Biol 72:339, 1977.

28. Rubino S, Fighetti M, Unger E, Cappuccinelli P: J Cell Biol 98:382, 1984.
29. Condeelis JS, Geosits S, Vahey M: Cell Motil 2:273, 1982.
30. Condeelis J, Vahey M, Carboni J, Demey J, Ogihara S: J Cell Biol 99:119s, 1984.
31. Condeelis JS, Salisbury J, Fujiwara K: Nature (Lond) 292:161, 1981.
32. Condeelis J, Hall A, Bresnick A, Warren V, Hock R, Bennett H, Ogihara S: Cell Motil, (in press).
33. Bonner JT, Hall EM, Sachsenmaier W, Walker BK: J Bacteriol 102:682, 1970.
34. Swanson JA, Taylor DL: Cell 28:225, 1982.
35. Janmey PA, Chaponnier C, Lind SE, Zaner KS, Stossel TP, Yin HL: Biochemistry 24:3714, 1985.
36. Bryan J, Coluccio LM: J Cell Biol 101:1236, 1985.
37. Giffard RG, Weeds AG, Spudich JA: J Cell Biol 98:1796, 1984.
38. Sha'afi RI, Shefcyk J, Yassin R, Molski TFP, Volpi M, Naccache PH, White JR, Feinstein MB, Becker EL: J Cell Biol 102:1459, 1986.
39. Europe-Finner GN, Newell PC: J Cell Sci 82:41, 1986.
40. Klein P, Fontana D, Knox B, Theibert A, Devreotes P: Cold Spring Harbor Symp Quant Biol 50:787, 1986.
41. Korn E: Physiol Rev 62:672, 1982.
42. Yumura S, Mori H, Fukui Y: J Cell Biol 99:894, 1984.
43. Janmey P, Stossel T: Nature 325:362, 1987.
44. Barak LS, Yocum RR, Webb WW: J Cell Biol 89:368, 1981.
45. Brenner M, Thoms SD: Dev Biol 101:136, 1984.